Atmospheric Research 95 (2010) 186–196

Contents lists available at ScienceDirect

Atmospheric Research

journal homepage: www.elsevier.com/locate/atmos

Pre-monsoon aerosol optical properties and spatial distribution over the Arabian Sea during 2006

M.C.R. Kalapureddy *, P.C.S. Devara

Indian Institute of Tropical Meteorology, Pashan, Pune 411 008, India

ARTICLE INFO

Article history:
Received 19 October 2008
Received in revised form 22 September 2009
Accepted 24 September 2009

Keywords:
AOT
Angstrom exponents
Arabian Sea
ICARB
Pre-monsoon

ABSTRACT

This paper presents the results of ship cruise and land observations of columnar aerosol characteristics over the Arabian Sea (AS) and at an in-land urban station Pune, in the western part of India, during the pre-monsoon 2006. Aerosol loading is found to decrease significantly from Pune and west coast of India to far away from the Indian west coast over AS. Relative dominance of coarse-mode particles is observed over pristine oceans, while dominance of fine-mode aerosols is noticed under certain occasions. Curvature of multi-spectral AOT variations is also found to be larger over Far AS (FAS) and Mid AS (MAS) regions, where the aerosol loading seems to be very low, compared to that over Coastal AS (CAS) region. Predominance of coarse- and fine-mode aerosols is found over Northern AS (NAS) and Southern AS (SAS) regions, respectively, along the meridional direction of AS. Surface radiative cooling due to aerosols is found to be more intense over CAS and NAS regions. It is shown that the combination of Angstrom exponent (α) and its second order (α') could delineate aerosol type and loading.

1. Introduction

The climate forcing by aerosols cooling effect could offset the greenhouse warming effect over large areas or could even delay the detection of greenhouse warming. The atmospheric aerosols may be of natural origin such as the wind-blown mineral dust or of anthropogenic origin such as those from industry, automobiles or other human activities in the urban areas. They may originate from gas-phase reactions of low volatile vapors in the atmosphere (Hoffmann et al., 1997). The natural aerosols, due to their dominant share (80%), evidently play a vital role in global-scale climate whereas anthropogenic aerosols play crucial role in regional-scale climatic features (e.g., Charlson et al., 1992; Satheesh et al., 1999; Ramanathan et al., 2001; Satheesh and Moorthy, 2005). Further, Ramanathan et al. (2005) have shown that a large reduction of solar radiation reaching the Earth's surface by anthropogenic aerosols. So, it is required to delineate the effects of natural and anthropogenic aerosols as far as regional features are concerned. Continents surrounding the AS and the North Indian Ocean (NIO) are responsible for the production of a variety of natural and anthropogenic aerosols. These aerosols and trace gases are advected to the oceanic regions over long distances depending on the prevailing source strengths and wind conditions. They remain in the marine atmosphere from a few days to few weeks until they lost into the ocean by gravitational settling or rain washout. In contrast to well-mixed greenhouse gases, aerosols exhibit large spatial and temporal variations and are responsible for producing large spatial inhomogeneity in the surface reaching solar flux intensity (e.g., Satheesh and Ramanathan, 2000). As the solar energy amount over the oceanic regions is one of the most important factors that drives the Earth's climate, understanding of the optical properties of aerosols and quantifying their radiative forcing form an important discipline in the climate change studies.

The well established linkage of dynamic and thermodynamic features, such as setting up of land–ocean thermal gradients (Asnani, 1993), low level jet (e.g., Findlater, 1969; Kalapureddy et al., 2007), and mini-warm pool over the south-east part of AS (e.g., Rao and Sivakumar, 1999), are associated with AS during the pre-monsoon which influences the ensuing

* Corresponding author.
E-mail address: kalapureddy1@gmail.com (M.C.R. Kalapureddy).

0169-8095/$ – see front matter © 2009 Elsevier B.V. All rights reserved.
doi:10.1016/j.atmosres.2009.09.014

monsoonal features, around May, over the Indian subcontinent. During pre-monsoon, the mean wind over the oceanic regions around the Indian sub-continent is northwesterly in direction. So, AS region could be a natural laboratory for assessing the role of aerosols during pre-monsoon. Hence, besides dynamic and thermodynamic linkages, the role of pre-monsoon aerosols over AS region is also expected to play a critical role, mainly, on the monsoon features over the Indian subcontinent (e.g., Devara et al., 2003) and partly on the global climate through radiation budget. Therefore, a good knowledge of pre-monsoon aerosol characteristics over the AS is important.

Recently, Indian Space Research Organization-Geosphere Biosphere Programme (ISRO-GBP) organized a nation-wide campaign, the so-called Integrated Campaign for Aerosols, gases and Radiation Budget-2006 (ICARB06), during March–May 2006 (Moorthy et al., 2008). This campaign comprises of three main segments viz., land, air and ocean. The ocean segment of the observational campaign covered extensively the marine region around the Indian sub-continent including both east and west coastal regions, Bay of Bengal (BoB) and AS. The broad features of aerosols over the BoB and AS observed during this campaign were discussed in our earlier paper (Kalapureddy and Devara, 2008). The present study compares and brings out an important contrast between BoB and AS aerosols together with a plausible explanation. Moreover, we focus here on investigating the aerosol optical and physical characteristics over the various parts of AS, (coastal, mid and far AS regions along zonal and northern and southern AS regions along meridional), and at a continental station (Pune) in the western part of India, during the pre-monsoon season of 2006. The spatial distribution in spectral characteristics of columnar AOT and α-Angstrom exponent and other observed parameters along the ship cruise over the AS were utilized to differentiate the aerosol types and properties over various locations in the AS.

2. Description of observations, database and methodology

Aerosols and radiation observations over the AS were made, with a fairly good time resolution (10 min interval), onboard Oceanographic Research Vessel Sagar Kanya (SK), on its cruise SK223 during the pre-monsoon season of 2006. Detailed description on the observations has been given in Kalapureddy and Devara (2008). In the present study, data archived around the western part of India and adjoining regions of AS only have been considered. The second leg (SK223B) observation started from the west coast (after the end of first leg on 12 April) from Cochin port (9.9°N, 76.2°E), on 18 April to cover AS regions and ended at Goa port (15.4°N, 73.8°E) on 11 May. For better understanding of spatial distribution of aerosol features, the entire AS is divided into three sub-regions, a) Coastal AS (CAS), less than 220 km from the coast, b) Mid AS (MAS), between 220 km and 550 km, and c) Far AS (FAS), above 550 km away from the Indian west coast. Besides this longitudinal bifurcation, latitudinal division is also made as Southern AS (SAS; 8–15°N) and Northern AS (NAS; 16–22°N). The cruise track of SK223 for ICARB06 for the entire period, 09 March–11 May 2006, is displayed in Fig. 1. The points on the track show the position of the ship at 0530 UTC on each day and the arrowhead shows its direction of movement along the track. For the same period, measurements made at an urban, in-land station Pune (18.3°N, 73.5°E), were also considered for comparisons. Pune is situated on the lee side of the Western Ghats and is about 100 km inland from the west coast of India (Fig. 1). The experimental site is located at an elevation of 570 m Above Mean Sea Level (AMSL) and is surrounded by hillocks as high as 760 m AMSL, forming a valley-like terrain. Water-soluble, dust-like and soot-like aerosols normally prevail over this station. In general, during the pre-monsoon season (March–May), the weather over and around the India is very hot with day's maximum temperature around 40 °C, while the surface winds are mostly gusty. The dust content in the atmosphere is at its maximum, and cumulonimbus clouds develop around the late afternoon to evening hours. Development of low-pressure system due to increased heating over land starts over India in the pre-monsoon, when all over India has the same pressure distribution, with only slightly higher pressure over the AS.

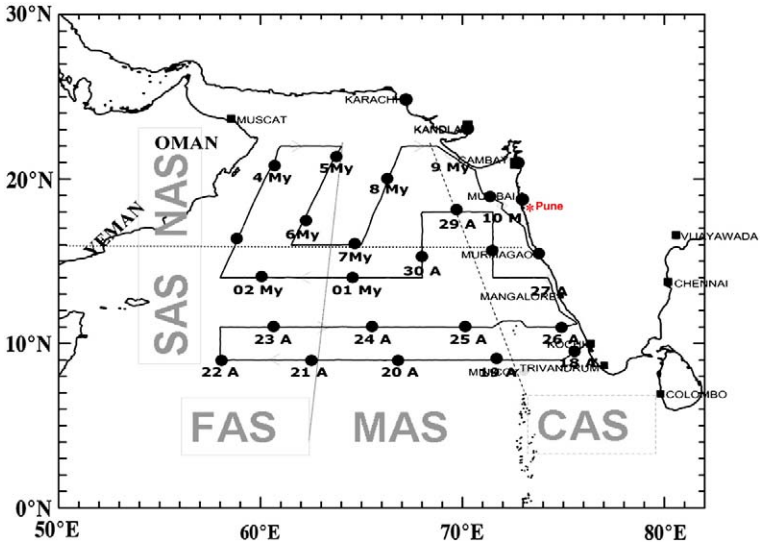

Fig. 1. Cruise track for ICARB06 during 09 March to 11 May 2006.

Observations on aerosol and trace gases were made using two (Sun photometer and Ozonometer) hand-held Microtops (Microprocessor-controlled total ozone portable spectrometer II; Solar Light Company, USA) (see Ichoku et al., 2002 for details). The Microtops (MT) provide columnar Aerosol Optical Thickness (AOT) at wavelengths centered at 340, 440, 500, 675, 870 and 1020 nm (with a full width half maximum band width is 5–10 nm), columnar water vapor (CWV) and columnar ozone derived from instantaneous solar flux measurements using its internal calibration; the typical error in AOT measurement using a Microtops Sun photometer is 0.03 (Ichoku et al., 2002). The field of view (FOV) of the MT is 2.5°. A Global Positioning System (GPS) receiver attached with the photometer provides the information on time and location. The down-welling Short Wave (SW) radiation measurements have also been made using Pyranometer (global Pyranometer, Weathertech. Co., India). Gimbals were used for on-board installation of the Pyranometer to compensate for rolling and pitching of the ship. Triplet observations were made at 10 minute-intervals to minimize the possible manual error in pointing the Sun from the moving platform. Besides independent calibration of the instruments prior to their deployment over the ship, an inter-calibration between MTs, operated from ship by different organizations was conducted to re-ensure the reliability of measurements. However, MT was not operated during around cloud passage on or near FOV facing the Sun. Thus, the observations were possible only for 24 days, and around 4500 observations recorded during the entire cruise period over AS. On a few occasions, over pristine oceans, the columnar AOT_{500} values were noted to be very low (<0.15 for 500 nm) especially over FAS region. Table 1 presents the details of observations made over the AS on 12 April and from 18 April to 10 May 2006 and those made over Pune during March–May 2006.

The Angstrom exponent α, can be computed via Volz method (Eck et al., 1999; 2001) using AOT (τ) observations at two wavelengths as:

$$\alpha = -d\ ln\ \tau_\lambda / d\ ln\ \lambda = -ln(\tau_{\lambda 2}/\tau_{\lambda 1}) / ln(\lambda_2/\lambda_1). \quad (1)$$

The difference in α computed in narrow spectral bands at shorter ($\alpha_{340-440}$) and longer ($\alpha_{675-870}$) wavelengths using Voltz method shows some promise in assessing the curvature (e.g., Kaskaoutis et al., 2007). The variation in α with wavelength is a more precise empirical relationship between aerosol extinction and wavelength, when it is simulated by a second-order polynomial fit (e.g., Eck et al., 1999; 2001; Pedros et al., 2003; Kaskaoutis and Kambezidis, 2006):

$$ln\ \tau_\lambda = \alpha_0 + \alpha_1 ln\lambda + \alpha_2 (ln\lambda)^2 \quad (2)$$

where α_2 accounts for a curvature observed with Sun photometry measurements. The derivative of Eq. (1) with respect to $\ln\lambda$ provides the second order Angstrom exponent (α'), which is equal to $-2\alpha_2$ (after substituting Eq. (2) in Eq. (1)). This curvature can be an indicator of aerosol particle size, with negative curvature indicating aerosol size distributions dominated by fine-mode and positive curvature indicating size distributions with significant contribution by the coarse-mode (Eck et al., 1999, 2001; Reid et al., 1999; Schuster et al., 2006). This second derivative constitutes a measure of the rate of change of the slope with respect to wavelength. Eck et al. (1999) attempted to quantify the curvature of the AOT curve using the second derivative of $\ln\tau_\lambda$ versus $\ln\lambda$, i.e., derivation of α with respect to $\ln\lambda$:

$$\alpha' = \frac{d\alpha}{dln\lambda} = -\left(\frac{2}{ln\lambda_{i+1} - ln\lambda_{i-1}}\right)\left(\frac{ln\tau_{a_{i+1}} - ln\tau_{a_i}}{ln\lambda_{i+1} - ln\lambda_i} - \frac{ln\tau_{a_i} - ln\tau_{a_{i-1}}}{ln\lambda_i - ln\lambda_{i-1}}\right) = -2\alpha_2. \quad (3)$$

α' close to zero indicates constant slope of the spectral AOT, indicating coarse-mode dominance, while a higher value represents rapidly changing slope. In the present study α' has been derived using observed AOT at 340, 500 and 1020 nm wavelengths.

3. Results and discussions

3.1. Observed background meteorological conditions

It is known that both dynamics and thermodynamics invariably play a vital role on aerosol load and its variation at any place. The aerosol loading at any location is generally influenced by the air mass and trajectories associated with the region for a particular period of time i.e., season. Satheesh and Srinivasan (2002) discussed the transport of Sahara desert dust over AS by means of northwesterly winds, and reported that the major fraction of the aerosols over AS is of desert dust of natural origin. In the present study also similar

Table 1
Some details of data archived during the ship cruise over various Arabian Sea regions and Pune in the western India.

Parameter(s) and instrumentation	Region	Clear sky observational days	Remarks
Microtops-II (Sun photometer and Ozonometer)	North AS	April 28–29; May 03–10	Useful data of 14 days
	South AS	April 12,18–27,30; May 01–02	Useful data of 10 days
	Coastal AS	April 12,18,25–28; May 09,10	Useful data of 08 days
	Mid AS	April 19,20,24,29,30; May 01,07,08	Useful data of 08 days
	Far AS	April 21–23; May 02–06	Useful data of 08 days
	Pune (an Indian west coast in-land station)	March–May 2006	Useful data of 28 days; 10 min. interval observations are only around 1½ hr of post-sunrise and pre-sunset and 30 min. interval for rest of the day

pre-monsoon wind features were noticed over the AS (see Fig. 2A); however, the surface wind speed is in the range of 6–9 m s^{-1} and wind direction is mostly north and/or southwesterly with strongest winds (~13 m s^{-1}) were noticed on 27 April near to Indian coast (near Mangalore) (not shown). Fig. 2B shows five-day back trajectories (at three altitudes) for the entire cruise period over AS obtained from NOAA HYSPLIT [National Oceanic and Atmospheric Administration Hybrid Single-Particle Lagrangian Integrated Trajectory version 4 (Draxler and Hess, 1998)] model. It is clearly revealed that different air masses (originating from west Asian, Indian, African and oceanic regions) influenced the AOT over AS. This analysis further showed that the African and Arabian air masses are also playing a significant role, besides Indian air mass, over the AS especially over FAS and NAS regions. In addition, the Indian land mass and oceanic air masses of NIO are also found to be influencing the MAS and CAS regions. The day-to-day back trajectory analysis revealed significant changes, which are considered to be responsible for the observed day-to-day variability of aerosol properties. Fig. 2 shows that in all cases, the lower altitude air masses originate from AS itself without traveling over longer distances while those at higher altitudes travel longer distance and affect significantly the trajectory direction on certain days (either from Indian subcontinent and/or from arid regions in south Asia and Arabian peninsula).

3.2. Spectral AOT variations

Time series of the daily mean values of columnar aerosol parameters (AOT_{500}, Angstrom exponent, curvature, α_2) obtained from Microtops' spectral AOT data are presented in Fig. 3. The ship-based observations of AOT_{500} with the satellite, Moderate Resolution Imaging Spectroradiometer's (MODIS) Aqua and Terra, daily observations of AOT_{550} are also compared (see Fig. 3A). For this AOT comparison, high-resolution MT observations were averaged for the entire observations in a day in order to match with daily MODIS observation. The daily AOT_{550} observed by Aqua and Terra has been collected for corresponding geographical position of

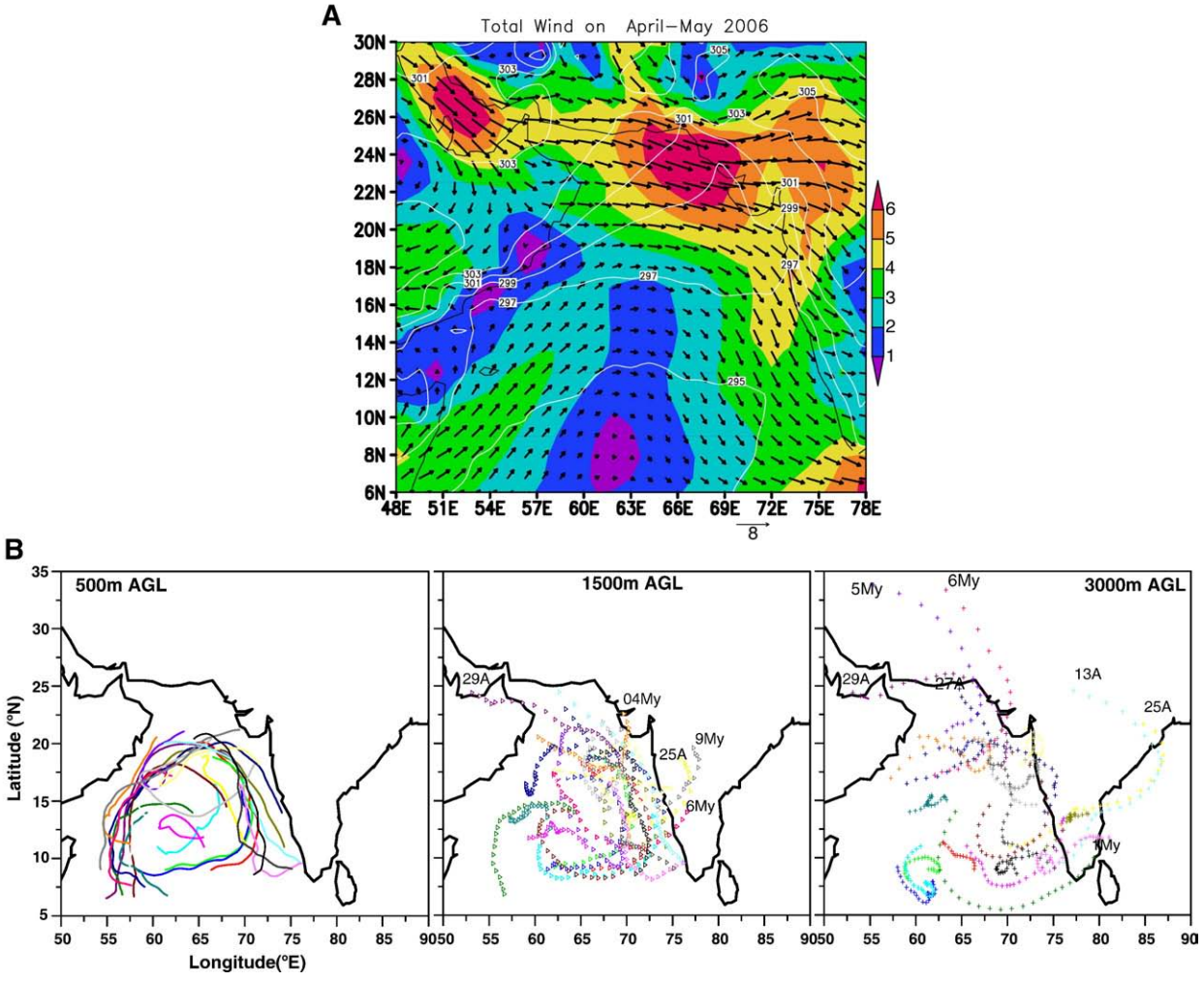

Fig. 2. A: ECMWF wind at 850 hpa over AS region during April–May 2006. B: 5-day HYSPLIT back trajectories over AS at (a) 500 m (b) 1500 m (c) 3000 m during 12 April to 10 May 2006.

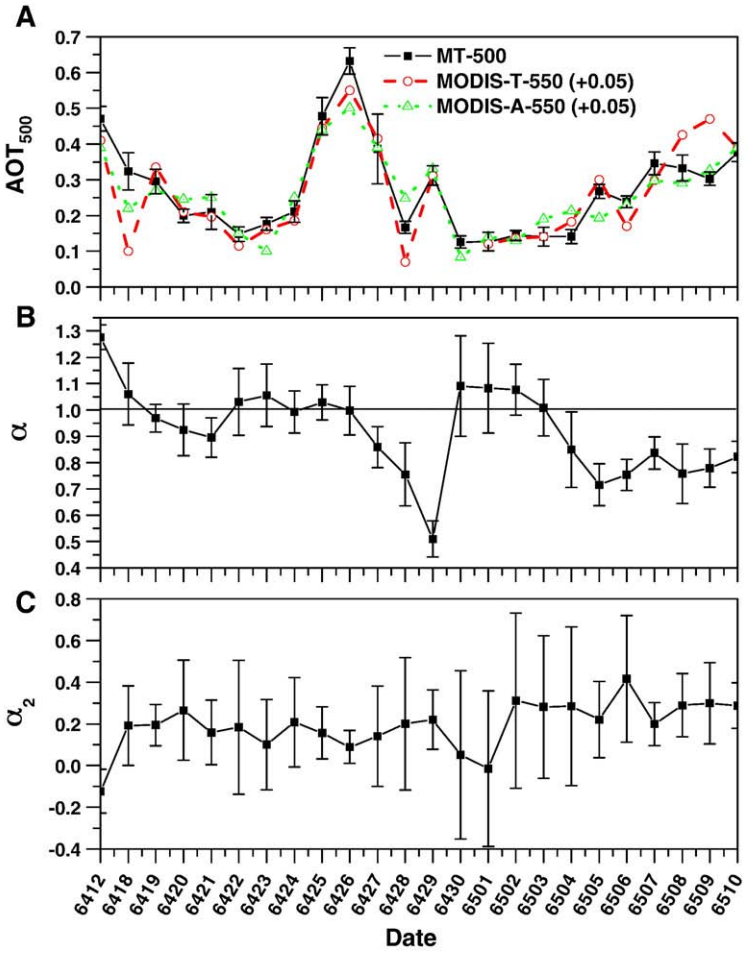

Fig. 3. Time series of the daily average values of (A) Microtops observed AOT_{500} compared with MODIS Aqua and Terra daily AOT_{550} (plus sign in bracket indicates the underestimation) (B) Angstrom exponent, α (C) Curvature, α_2.

the present ship based daily mean MT observation of AOT_{500}. The slight underestimation (of order 0.05) was found with satellite relative to our observations. Otherwise, the comparison is found to be reasonably good with a correlation coefficient of above 80%. Except around 26 April (near Mangalore coast) the AOT_{500} values over AS are low, varying in between 0.10 and 0.35. Higher AOT_{500} values (~0.7) over Mangalore coast seem to be a regular feature, over this region, from the knowledge of present and earlier cruises reports (e.g., Ramachandran, 2004). Time series of α observation show higher values in the beginning and lower at the ending of the cruise with a sharp fall in α values during 27–29 April which was found to be associated with air mass trajectories originating from Persian Gulf and Arabian Peninsula (see Fig. 2B). The mean values of AOD_{500} and $\alpha_{340-1020}$ are 0.25 ± 0.11 and 0.90 ± 0.19 respectively. Earlier studies over the AS region also report the near similar AOD_{500} (~0.3) and α (~1) during around pre-monsoon (March–May) season [e.g., Satheesh et al., 1999; Moorthy et al., 2001; Ramanathan et al., 2001; Li and Ramanathan, 2002; Babu et al., 2008]. From low α values and back trajectories analysis, it can be understood that there was a rather significant desert-dust aerosol contribution during 27–29 April originating from long distant semi-arid regions besides the locally generated coarse-mode (shorter life) sea salt aerosols, which seems to be uniform for all the observational days (see Fig. 2). Nevertheless, the absence of low α values, during the campaign, differentiates AS from other oceanic regions. It has also found that the sea salts contribution is around 20% over AS during the campaign. This has attributed to the weak sea-salt production because of low surface wind speeds over the region during the campaign [see Nair et al., 2008]. The curvature, α_2, shows mostly positive values indicating the significant contribution of coarse-mode aerosols in the size spectrum. It can be noted that α_2 and, as a consequence, α' values show relatively higher standard deviation when the AOT_{500} values were critically below 0.15. It may be noted here that under such low turbid conditions, the uncertainty associated with the computed α_2 and α' through the polynomial fit (Eqs. (1) and (2)) will be more and hence their physical significance, during such conditions, can be less reliable. This was also apparent in numerous studies since the above retrievals deal with greater uncertainties under low turbid conditions. This fact is always the case, nearly independent from the instrumentation used, while extensive analysis and explanations for these errors are given in Kaskaoutis et al. (2006). However, in general, they provide reliable information

about the type of aerosols to the aerosol size distribution under sufficiently high aerosol loading environments.

The spatial distribution of MT-observed AOT_{500}, Angstrom exponent ($\alpha_{340-1020}$), second order Angstrom exponent (α) and columnar water vapor (CWV) over AS during the pre-monsoon 2006 are shown in Fig. 4(A–D). High AOT values were observed along the Indian west coast and lower values along the FAS region. Secondary maximum in AOT, noticed over northern part of CAS with the primary maximum at Mumbai coast could be due to the air mass advected from land region. Similar results were also noticed during INDOEX (e.g., Moorthy et al., 2001). Mostly lower AOT values were noticed over pristine oceanic regions over central and western parts of AS. The wavelength exponent $\alpha_{340-1020}$ shows higher values in the central and western parts of AS where AOT found to be relatively low. Furthermore, the Angstrom exponent shows lower values over northern AS compared to southern AS. This indicates the dominance of coarse-mode aerosols in the size spectrum which may have originated from near-by desert sources (Thar and Arabian deserts). We also noticed a significant latitudinal gradient in observed CWV with relatively drier northern part than the southern part of AS. For better understanding of this feature, the MODIS-Terra time averaged values with a spatial resolution of $1^\circ \times 1^\circ$ (Level 3) for the observational period (10 April–10 May) and coordinates (8–22°N; 56–76°E), associated with the AS region are examined in Fig. 5. For this we rationally choose parameters in association with Fig. 4 such as mass concentration (MC) alternative for aerosol load, small mode fraction (SMF) alternative for α, aerosol effective radius (R_{eff}) alternative for α' along with water vapor observations of satellite and are presented in Fig. 5. Even though this figure was obtained from the area averaged for 30 days, which could essentially smooth out local or short-lived events, it nearly coincides with our ground-based results shown in Fig. 4. The Fig. 5 confirms that the high aerosol concentrations occur near to the Indian coast and northern AS with lower concentrations pertain to southwestern part of AS along with secondary maximum concentration near northern part of CAS region. Combined SMF and R_{eff} reveals the presence of coarse-mode aerosols (>0.6 μm) over northern part of AS where the CWV show relatively low values. Hence both ground-based and satellite observations (Figs. 4 and 5) revealed significant latitudinal gradients in the AOT and water vapor over the AS region with higher aerosol load and less water vapor in the northern AS where the coarse-mode aerosols are found dominant. Besides these, there also exist significant longitudinal gradients in aerosol features as presented in Table 2. It infers that, from the western part of India, aerosol turbidity (loading) decreases while moving towards far west of Indian coast. Lower values of α are seen over Pune and near constant values are observed over the three zonal regions of AS. Both of α and α' together show lower magnitudes closer to the western part of India (either at CAS region or Pune), which implies relatively coarse-mode dominance over the CAS and Pune, whereas fine-mode aerosols over the MAS and FAS regions dominate. This is consistent because winds flow from north-westerly direction during the pre-monsoon months to monsoon transition period, which brings significant marine air-mass rich in coarse-mode particles to Pune as reported in the literature (Devara et al., 2005).

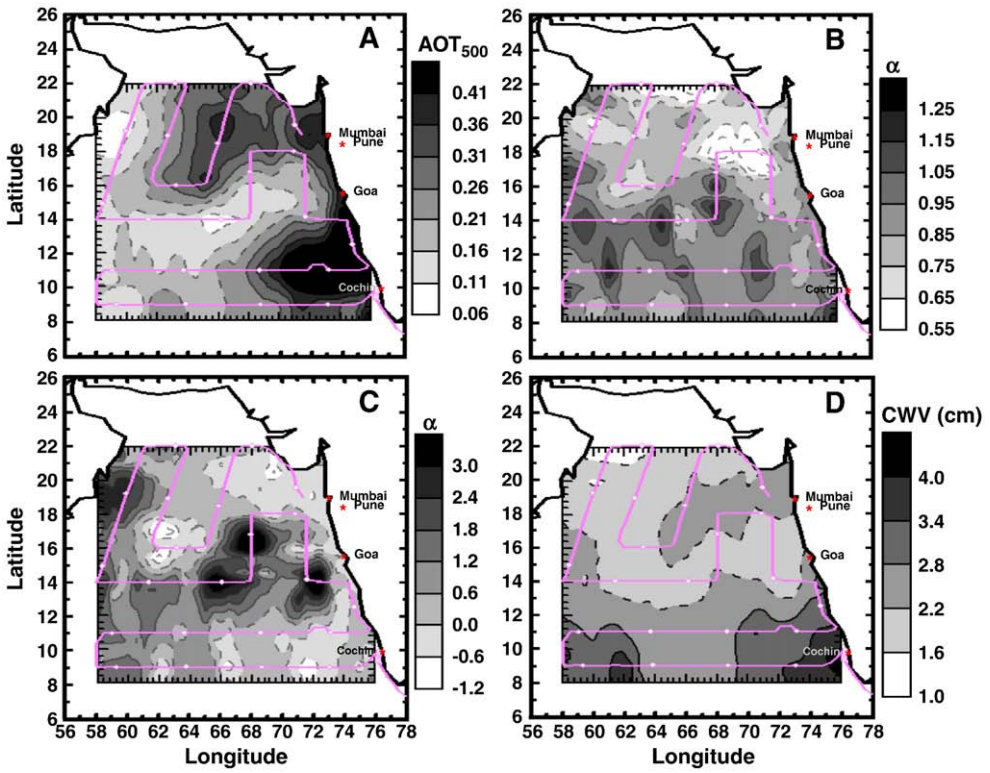

Fig. 4. Spatial distribution of (A) AOT_{500}, (B) Angstrom exponent ($\alpha_{340-1020}$) (C) Second derivative of Angstrom exponent (α') (D) column water vapor observed over Arabian Sea region during 12 April to 10 May 2006. Cruise track shown in pink line.

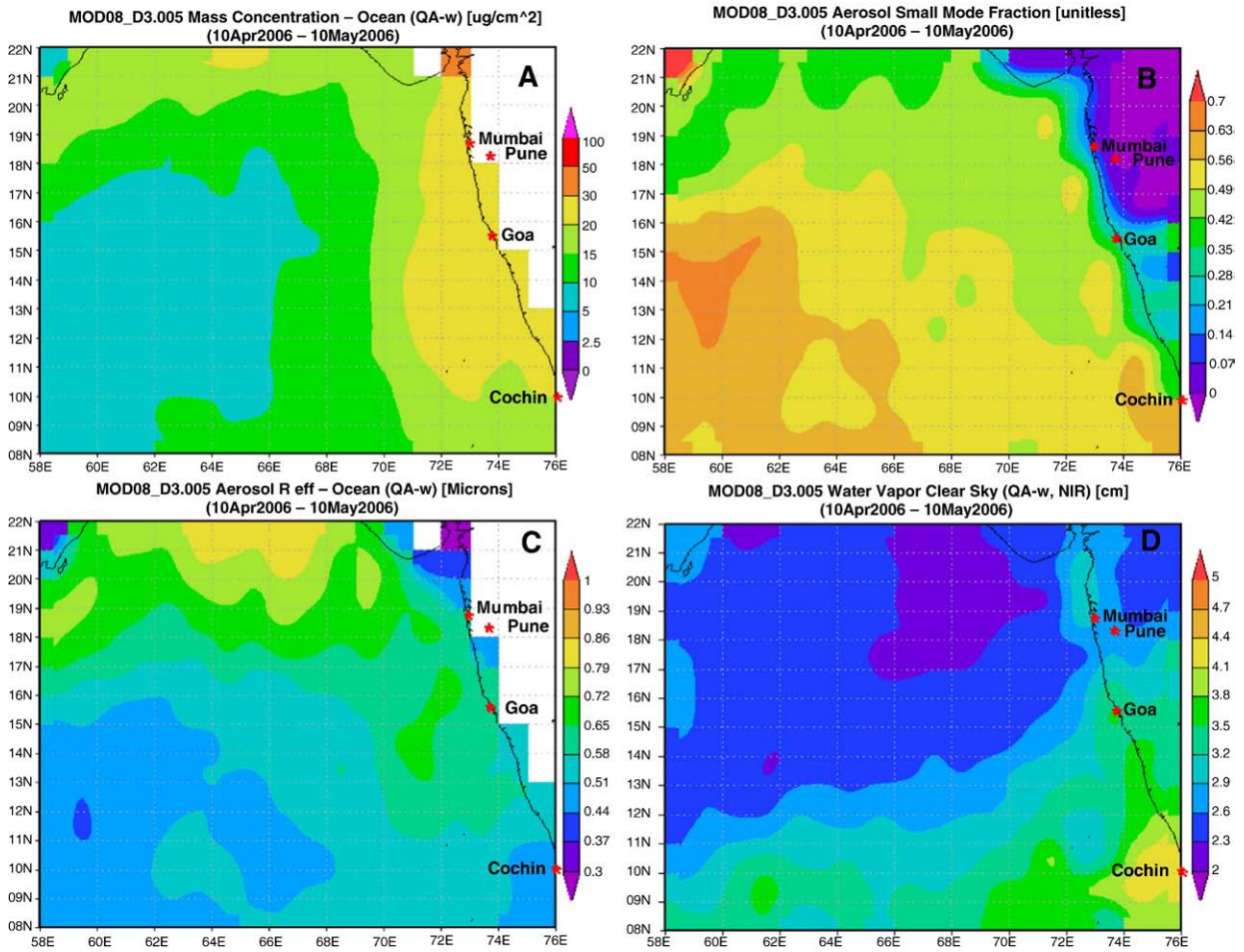

Fig. 5. MODIS observed (A) Mass concentration (B) Small Mode Fraction (C) Effective Radius (D) water vapor distribution of over AS during 10 April–10 May 2006.

Fig. 6(A–C) shows the mean spectral variation of AOT over various parts of AS [zonal (CAS, MAS and FAS) and meridional (SAS and NAS)] and inverted size distributions of aerosols (ASD) following the constrained liner numerical inversion scheme as suggested by King et al. (1978) and King (1982). Aerosol turbidity shows clear meridional (longitudinal) variation with maximum in CAS and minimum in FAS whereas this was less significant in the zonal (latitudinal). Over AS, all the regions exhibited similar spectral variation of AOT which resulted in near equal values of α. It is interesting to notice a significant increase in AOT values above 500 nm in the NAS region compared to SAS region. This is an indication of significant increase of coarse-mode particles in the NAS region. This significant change in spectral AOT features along the North–South direction of AS lead to have different α values over NAS and SAS regions with coarse (fine) mode dominance over NAS (SAS) region. Moreover, CAS and NAS regions show near zero or negative values of α' indicating the increased coarse-mode aerosol contribution in the size distribution. In addition, a sudden fall (about 30%) is observed from AOT_{340} to AOT_{440}, and thereafter a small increase in AOT_{500} points out the possible existence of bi-modal ASD (see Fig. 6B) constituting natural or coarse-mode particles over the AS. In order to estimate ASD, mean spectral AOT values for forenoon (FN) and afternoon (AN) of each day were used by inverting the spectral variation of AOT using the constrained linear

Table 2
Mean values of different parameters during the ICARB06 over various Arabian Sea regions and Pune in western India.

Region	AOT_{500}	$\beta \pm$ S.D.	$\alpha \pm$ S.D.	α'	$\Delta F^{\#*}$ (R^2,N) (W m^{-2})
North AS	0.26 ± 0.08	0.15 ± 0.05	0.76 ± 0.15	-0.05 ± 0.98	-34.0 ± 2.9(0.87,45)
South AS	0.25 ± 0.14	0.12 ± 0.07	1.03 ± 0.15	0.78 ± 1.16	-24.2 ± 1.8(0.87,55)
Far AS	0.18 ± 0.05	0.09 ± 0.04	0.91 ± 0.17	0.49 ± 1.21	-22.0 ± 3.2(0.50,49)
Middle AS	0.23 ± 0.09	0.13 ± 0.06	0.88 ± 0.24	0.53 ± 1.28	-22.1 ± 1.4(0.75,79)
Coastal AS	0.36 ± 0.12	0.18 ± 0.05	0.91 ± 0.18	0.08 ± 0.82	-34.2 ± 1.0(0.96,51)
PUNE	0.35 ± 0.08	0.20 ± 0.04	0.67 ± 0.17	0.16 ± 0.10	Not known

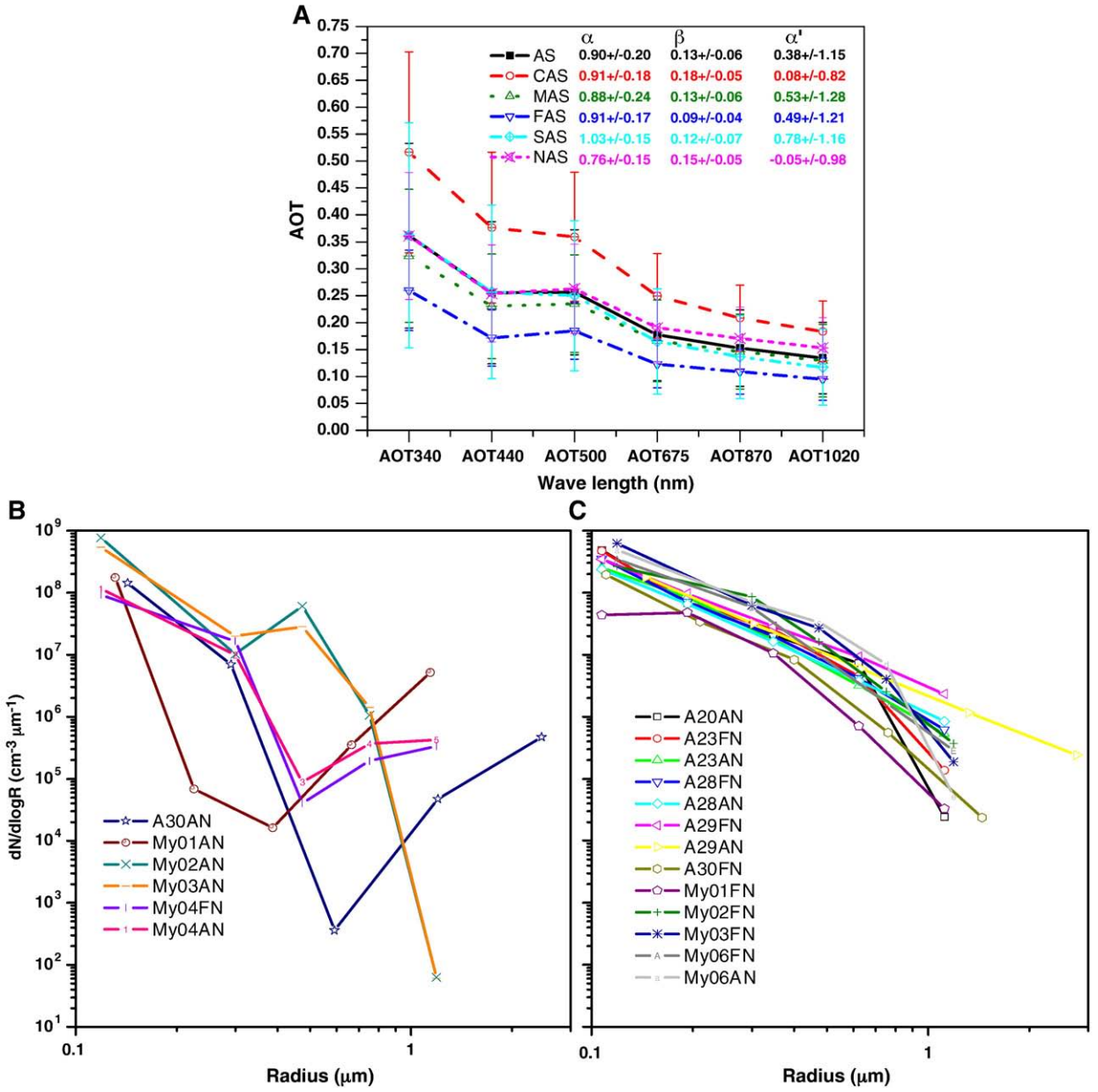

Fig. 6. Spectral characteristics of AOT over (A) various regions of Arabian Sea along longitude and latitude viz., Far, Middle, and Coastal AS and Southern and Northern AS (see text for details) (B and C) Inverted Aerosol Size Distribution seen over the Arabian Sea (FN: Forenoon; AN: Afternoon).

inversion scheme (as explained in Section 2). The columnar ASD estimated for a few typical days are shown in Fig. 6(B–C). Most of the time, either power law or mono-modal distribution was noticed. The bi-modal distributions (Fig. 6B) observed in the afternoon period were mostly found associated with the MAS and FAS regions, indicating the dominance of coarse-mode contribution in those regions. Further, bi-modal distribution noticed in the pristine oceans during the presence of north westerly winds. Relatively lower β (aerosol loading) with higher α values were noticed on few clear sky days over pristine oceanic regions far away from west coast of India indicating fine-mode dominance in the aerosol size spectrum. These values are also noticed to be relatively lower over AS than those over BoB during this campaign (Kalapureddy and Devara, 2008) implying that the AS is relatively cleaner than the BoB region during the pre-monsoon, which is mostly due to the prevailing wind conditions, air mass trajectories and large scale circulation pattern associated with those regions. Hence, Fig. 6 clearly shows that there exists a significant change in aerosol turbidity along zonal (arising either due to aerosol concentration or due to more hygroscopic nature of aerosols) whereas in meridional belt there was a significant change in spectral AOT features (indicating a change in aerosol type) over AS. These features were discussed further in the next section using spectral curvature.

3.3. Angstrom parameters

In Fig. 7, (from left to right CAS, MAS, FAS, SAS and NAS regions respectively), the top panels show the difference of α at shorter ($\alpha_{340-440}$) and longer ($\alpha_{675-870}$) wavelength intervals with respect to turbidity, by means of AOT_{500}. The points on negative and positive differences correspond to negative and positive α_2 values, respectively. In case of positive curvature ($\alpha_2 > 0$, concave type curves on $\ln\tau$ vs $\ln\lambda$ plot) the rate of change of α is more significant at the shorter wavelengths and vice versa. The existence of positive curvature conforms the coarse-mode dominance over all the regions in the AS as evident from Fig. 7. Furthermore, NAS region shows predominant coarse-mode aerosols since nearly the whole data points lying in the positive curvature region. In all the regions the regression between α in the two spectral intervals is not linear, as revealed by the very small fraction of total points lying on the one-to-one line. Kaskaoutis et al. (2007) reported that the curvature does not depend on the slope of the straight line of $\ln\tau$ versus $\ln\lambda$ considered in either at shorter or longer wavelengths but depend on the differences in α computed at shorter and longer wavelengths. Positive (negative) difference is indicative of positive (negative) curvature, while differences near zero indicate the absence of spectral variability in the Angstrom exponent (Schuster et al., 2006). However, Kaskaoutis et al. (2007) showed that the above statement is valid only in cases in which the differences and the curvature are computed in the same spectral interval. Further, significant fine-mode dominance was noticed over the Southern AS region whereas coarse-mode dominance was seen over the Northern and Coastal AS regions. It is also noticed (not shown) that the Angstrom exponent derived at different wavelength intervals resembles the reported desert-dust particles (Kaskaoutis et al., 2007) which also supports the present observation of predominance of coarse-mode aerosols over the AS. It can also be noted that at low turbid conditions ($AOT_{500} < 0.3$) differences in α at shorter and longer wavelengths exhibit wide range of magnitude, which may partly be associated with the computational uncertainty in retrieving α at low turbidity conditions. However, these differences reduce gradually with increasing AOT_{500}. The correlation between α' and turbidity by means of AOT_{500} can be seen in the bottom panels of the Fig. 7. Number of observations having $\alpha_{(340-1020)} < 1$ constitutes 77.4%, 68.3%, 67.8%, 42.6% and 93.7% of the total observations over CAS, MAS, FAS, SAS and NAS regions, respectively. Similarly for $\alpha' > 0$, the corresponding number of observations are 44.4%, 59.6%, 72.6%, 76.9% and 44.8%. This shows fine-mode dominance over the FAS and SAS regions and coarse-mode predominance over the CAS and NAS regions, which is considered to be due to the combined impact of land mass transport and local sea-salts. It is also noticed that in low turbid conditions ($AOT_{500} < 0.3$) the fine-mode particle dominance is significant in all over the AS. Over CAS and NAS regions, more than 90% of α' data just lie in between ± 1.5 whereas in the MAS and FAS regions α' variations are larger.

3.4. Surface radiative forcing

The Pyranometer-measured global SW flux in the wavelength region between 0.3 and 3.0 μm is correlated with instantaneous AOT_{500} (corrected to the air mass factor, $1/\mu$) so as to calculate the radiative forcing as reported by Jayaraman et al. (1998). Normalization of the AOT with μ ($=\mathrm{Cos}\ \theta$) is found to be necessary as the slant air column length increases with increasing solar zenith angle θ. The observed solar flux represents the solar flux at sea surface, normal to the angle of incidence, with a cone of about 2.5° around the Sun. The data for solar zenith angle greater than 60° are excluded (to avoid Earth's curvature effect) and the AOT/μ values are restricted to within 0.8. Fig. 8 shows scatter plot of the measured–normalized SW flux with AOT for specific zonal (CAS, MAS and FAS) and meridional (SAS and NAS) cross-sections of the study

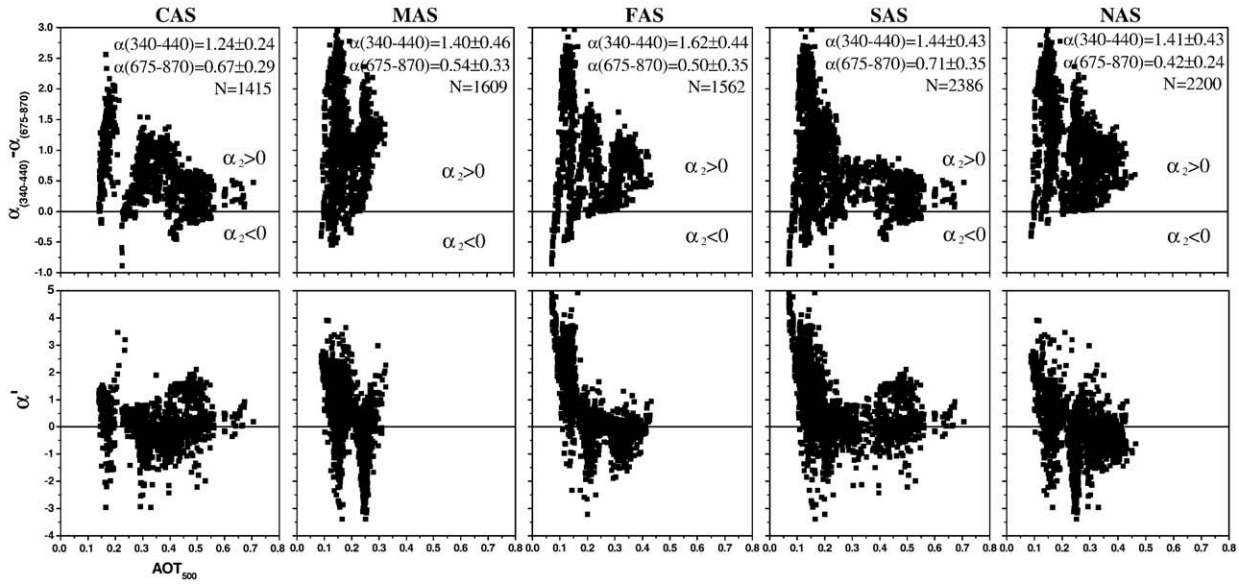

Fig. 7. Correlation plots of (top panels) difference of Angstrom exponent at shorter ($\alpha_{340-400}$) and longer ($\alpha_{675-870}$) wavelength with AOT_{500} (bottom panels) α' vs AOT_{500} for various regions over AS.

region. A straight line could be fitted with a negative slope of about 342, 221 and 220 W m^{-2} per unit AOT for CAS, MAS and FAS regions, respectively. It was noted to be 242 and 340 W m^{-2} per unit AOT for SAS and NAS regions, respectively (last column of Table 2 presents the regression analysis statistics related to it). This implies that for a 0.1 increase in the prescribed columnar AOT the sea-surface solar flux decreases by about 34.2, 22.1 and 22.0 W m^{-2} for CAS, MAS and FAS regions, respectively. This was about 24 and 34 W m^{-2} for SAS and NAS regions, respectively, in meridional AS. The above calculations mostly confined to fewer data sets which represent a specific region over AS. By considering all the observed days over AS, the average decrease in sea-surface solar flux over AS is about 18 W m^{-2} (Kalapureddy and Devara, 2008). This is near comparable to the surface solar flux values reported by Jayaraman et al. (1998) and Moorthy et al. (2005). The largest aerosol forcing at bottom of the atmosphere over the CAS and NAS regions, as expected, could be due to higher aerosol load, which attenuates the surface-reached solar irradiance over the Arabian Sea.

4. Conclusions

The pre-monsoon aerosol features studied during 2006 at Pune (land segment) and over the AS (ocean segment) revealed the following.

1. The average AOT_{500} showed minimum values in FAS region and increased from there to CAS region, towards west coast of India taking maximum values at western Indian land station, Pune. There was two-fold increase in AOT from FAS to Pune. The overall coarse-mode predominance was the general characteristics over the AS.
2. Latitudinal gradients in AOT and water vapor indicated higher aerosol loading with low water vapor situations over North AS region suggesting predominance of coarse-mode aerosols. This is mainly due to the long range transport of adjoining arid air-mass by the north westerly wind during the study period.
3. There exists a clear change in aerosol turbidity along zonal (indicate change in aerosol concentration or hydrophilic nature) whereas in meridional there was a substantial change in spectral AOT features (indicating change in aerosol type) over AS.
4. Combined α and α' values showed lower magnitudes close to western part of India (either at CAS region or Pune) which infers the relative coarse-mode dominance over CAS and Pune and fine-mode dominance over MAS and FAS regions. Diminishing of the fine-mode particles, from FAS to Pune, could be due to the background winds which mostly blow from pristine oceans during the period of study.
5. The sea surface solar flux (ΔF) over CAS, MAS and FAS regions showed increase radiative cooling at sea surface from FAS to CAS region from 22.0 to 34.2 W m^{-2}.

Acknowledgments

The work reported in this paper has been carried out under the ISRO-GBP-ICARB project. Authors are thankful to NCAOR/DOD for onboard facilities and also to the Sagar Kanya cruise members for their excellent co-operation. We are grateful to the anonymous Reviewers for their valuable comments and suggestions which helped in improving the scientific content of the paper. Thanks are also due to Director, and all Members of the Lidar and Radiometric Group, IITM for their cooperation. The authors also gratefully acknowledge the NOAA Air Resources Laboratory (ARL) for making available the HYSPLIT (http://www.arl.noaa.gov/ready.html) trajectories used in this paper. We also acknowledge with thanks the GES-DISC DAAC On-line Visualization and Analysis System: Web-based interface for the visualization and analysis of the MODIS data (http://g0dup05u.ecs.nasa.gov/Giovanni/).

References

Asnani, G.C., 1993. Tropical Meteorology. I and II, Pune, India.
Babu, S.S., Nair, V.S., Moorthy, K.K., 2008. Seasonal changes in aerosol characteristics over Arabian Sea and their consequence on aerosol short-wave radiative forcing: Results from ARMEX field campaign. J. Atmos. Solar Terr. Phys. 70, 820–834.
Charlson, R.J., Schwartz, S.E., Hales, J.M., Cess, R.D., Coakley Jr., J.A., Hansen, J.E., Hoffmann, D., 1992. Climate forcing by anthropogenic aerosols. Science 255, 423–440.
Devara, P.C.S., Raj, P.E., Pandithurai, G., Dani, K.K., Maheskumar, R.S., 2003. Relationship between lidar-based observations of aerosol content and monsoon precipitation over a tropical station Pune. India Meteorol. Appl. 10, 253–262.
Devara, P.C.S., Saha, S.K., Raj, P.E., Sonbawne, S.M., Dani, K.K., Tiwari, Y.K., Maheskumar, R.S., 2005. A four-year climatology of total column tropical urban aerosol, ozone and water vapour distributions over Pune, India. Aerosol Air Qual 5, 103–114.
Draxler, R.R., Hess, G.D., 1998. An overview of the HYSPLIT4 modeling system for trajectories, dispersion, and deposition. Aust. Meteorol. Mag. 47, 295–308.
Eck, T.F., Holben, B.N., Reid, J.S., Dubovik, O., Smirnov, A., O'Neill, N.T., Slutsker, I., Kinne, S., 1999. Wavelength dependence of the optical depth of biomass burning, urban, and desert dust aerosols. J. Geophys. Res. 104 (D24), 31333–31349.
Eck, T.F., Holben, B.N., Dubovik, O., Smirnov, A., Slutsker, I., Lobert, J.M., Ramanathan, V., 2001. Column-integrated aerosol optical properties over

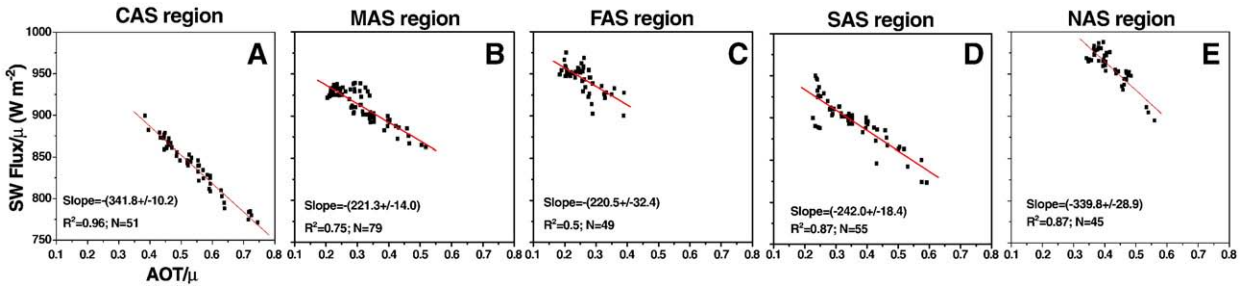

Fig. 8. Association between global solar flux and columnar AOT_{500} normalized for the air mass ($1/\mu$) over (A) Coastal AS (B) Mid AS (C) Far AS (D) Southern AS and (E) Northern AS regions during the cruise track of SK223B. A linear correlation is obtained by restricting AOT/μ within 0.8.

the Maldives during the northeast monsoon for 1998–2000. J. Geophys. Res. 106, 28555–28566.
Findlater, J., 1969. A major low level current near the Indian Ocean during northern summer. Q. J. R. Meteorol. Soc. 95, 362–380.
Hoffmann, T., Odum, J.R., Bowman, F., Collins, D., Klockow, D., Flagan, R.C., Seinfeld, J.H., 1997. Formation of organic aerosols from the oxidation of biogenic hydrocarbons. J. Atmos. Chem. 26, 189–222.
Ichoku, I., Levy, R., Kaufman, Y.J., Remer, L.A., Li, R.R., Mar-tins, V.J., Holben, B.N., Abuhassan, N., Slutsker, I., Eck, T.F., Pietras, C., 2002. Analysis of the performance characteristics of the five-channel Microtops II Sun photometer for measuring aerosol optical thickness and precipitable water vapor. J. Geophys. Res. 107 (D13). 4179. doi:10.1029/2001JD001302.
Jayaraman, A., Lubin, D., Ramachandran, S., Ramanathan, V., Woodbridge, E., Collins, W.D., Zalpuri, K.S., 1998. Direct observations of aerosol radiative forcing over tropical Indian Ocean during the January–February 1996 pre-INDOEX cruise. J. Geophys. Res. 103 (D12), 13827–13836.
Kalapureddy, M.C.R., Devara, P.C.S., 2008. Characterization of pre-monsoon aerosols over oceanic regions around India. Atmos. Environ. 42, 6816–6827. doi:10.1016/j.atmosenv.2008.05.022.
Kalapureddy, M.C.R., Rao, D.N., Jain, A.R., Ohno, Y., 2007. Wind profiler observations of a monsoon low-level jet over a tropical Indian station. Ann. Geophys. 25, 2125–2137. www.ann-geophys.net/25/2125/2007/.
Kaskaoutis, D.G., Kambezidis, H.D., 2006. Investigation on the wavelength dependence of the aerosol optical depth in the Athens area. Q. J. R. Meteorol. Soc. 132, 2217–2234.
Kaskaoutis, D.G., Kambezidis, H.D., Adamopoulos, A.D., Kssomenos, P.A., 2006. Comparison between experimental data and modeling estimates of aerosol optical depth over Athens, Greece. J. Atmos. Solar Terr. Phys. 1167–1178.
Kaskaoutis, D.G., Kambezidis, H.D., Hatzianastassiou, N., Kosmopoulos, P.G., Badarinath, K.V.S., 2007. Aerosol climatology: dependence of the Angstrom exponent on wavelength over four AERONET sites. Atmos. Chem. Phys. Discuss. 7, 7347–7397. http://www.atmos-chem-phys-discuss.net/7/7347/2007/.
King, M.D., 1982. Sensitivity of constrained linear inversions to the selection of the Lagrange multiplier. J. Atmos. Sci. 39, 1356–1369.
King, M.D., Byrne, D.M., Herman, B.M., Reagan, J.A., 1978. Aerosol size distributions obtained by inversion of spectral optical depth measurements. J. Atmos. Sci. 35, 2153–2167.
Li, F., Ramanathan, V., 2002. Winter to summer monsoon variation of aerosol optical depth over the tropical Indian Ocean. J. Geophys. Res. 107 (D16), 4284. doi:10.1029/2001JD000949.
Moorthy, K.K., Saha, A., Niranjan, K., 2001. Spatial variation of aerosol spectral optical depth and columnar water vapor content over the Arabian Sea and Indian Ocean during the IFP of INDOEX. Curr. Sci. 80, 145–150.
Moorthy, K.K., Suresh Babu, S., Satheesh, S.K., 2005. Aerosol characteristics and radiative impacts over the Arabian sea during the intermonsoon season: Results from ARMEX field campaign. J. Atmos. Sci. 62, 192–206.
Moorthy, K.K., Satheesh, S.K., Babu, S.S., Dutt, C.B.S., 2008. Integrated Campaign for Aerosols, gases and Radiation Budget (ICARB): an overview. J. Earth Sys. Sci. 117, 243–262.
Nair, V.S., Moorthy, K.K., Babu, S.S., 2008. Size segregated aerosol mass concentration measurements over the Arabian Sea during ICARB. J. Earth Sys. Sci. 117, 315–323.
Pedros, R., Martinez-Lozano, J.A., Utrillas, M.P., Gomez-Amo, J.L., Tena, F., 2003. Column-integrated aerosol, optical properties from ground-based spectroradiometer measurements at Barrax (Spain) during the Digital Airborne Imaging Spectrometer Experiment (DAISEX) campaigns. J. Geophys. Res. 108 (D18), 4571. doi:10.1029/2002JD003331.
Ramachandran, S., 2004. Spectral aerosol optical characteristics during the northeast monsoon over the Arabian Sea and the tropical Indian Ocean: 1. Aerosol optical depths and their variabilities. J. Geophys. Res. 109, D19207. doi:10.1029/2003JD004476.
Ramanathan, V., Crutzen, P.J., Lelieveld, J., Mitra, A.P., Althausen, D., Anderson, J., Andreae, M.O., Cantrell, W., Cass, G.R., Chung, C.E., Clarke, A.D., Coakley, J.A., Collins, W.D., Conant, W.C., Dulac, F., Heintzenberg, J., Heymsfield, A.J., Holben, B., Howell, S., Hudson, J., Jayaraman, A., Kiehl, J.T., Krishnamurti, T.N., Lubin, D., McFarquhar, G., Novakov, T., Ogren, J.A., Podgorny, I.A., Prather, K., Priestley, K., Prospero, J.M., Quinn, P.K., Rajeev, K., Rasch, P., Rupert, S., Sadourny, R., Satheesh, S.K., Shaw, G.E., Sheridan, P., Valero, F.P.J., 2001. Indian Ocean Experiment: an integrated analysis of the climate and the great Indo-Asian haze. J. Geophys. Res. 106 (D22), 28,371–28,398.
Ramanathan, V., Chung, C., Kim, D., Bettge, T., Buja, L., Kiehl, J.T., Washington, W.M., Fu, Q., Sikka, D.R., Wild, M., 2005. Atmospheric brown clouds: Impacts on South Asian climate and hydrological cycle. Proc. Natl. Acad. Sci. U. S. A. 102 (15), 5326–5333.
Rao, R.R., Sivakumar, R., 1999. On the possible mechanisms of the evolution of a mini-warm pool during the pre-summer monsoon season and the onset vortex in the southeastern Arabian Sea. Q. J. R. Meteorol. Soc. 125 (555 Part A), 787–809.
Reid, J.S., Eck, T.F., Christopher, S.A., Hobbs, P.V., Holben, B.N., 1999. Use of the Angstrom exponent to estimate the variability of optical and physical properties of aging smoke particles in Brazil. J. Geophys. Res. 104 (D22), 27473–27489.
Satheesh, S.K., Moorthy, K.K., 2005. Radiative effects of natural aerosols: a review. Atmos. Environ. 39, 2089–2110.
Satheesh, S.K., Ramanathan, V., 2000. Large differences in the tropical aerosol forcing at the top of the atmosphere and Earth's surface. Nature 405, 60–63.
Satheesh, S.K., Srinivasan, J., 2002. Enhanced aerosol loading over Arabian Sea during the pre-monsoon season: natural or anthropogenic? Geophys. Res. Lett. 29 (18), 1874. doi:10.1029/2002GL015687.
Satheesh, S.K., Ramanathan, V., Jones, X.L., Lobert, J.M., Pod-gorny, I.A., Prospero, J.M., Holben, B.N., Loeb, N.G., 1999. A model for the natural and anthropogenic aerosols for the tropical Indian Ocean derived from Indian ocean experiment data. J. Geophys. Res. 104, 27,421–27,440.
Schuster, G.L., Dubovik, O., Holben, B.N., 2006. Angstrom exponent and bimodal aerosol size distributions. J. Geophys. Res. 111, D07207. doi:10.1029/2002GL015687.